Multiple Input-Multiple Output Cycle-to-Cycle Control of Manufacturing Processes

Adam K. Rzepniewski*, David E. Hardt**

*Ph.D. candidate in the department of Mechanical Engineering at the Massachusetts Institute of Technology, Cambridge, MA 02139 USA; e-mail: adamr@ mit.edu.
** Professor of Mechanical Engineering at the Massachusetts Institute of Technology, Cambridge, MA 02139 USA.

Abstract— **Cycle-to-cycle control is a method for using feedback to improve product quality for processes that are inaccessible within a single processing cycle. This limitation stems from the impossibility or the prohibitively high cost of placing sensors and actuators that could facilitate control during, or within, the process cycle. Our previous work introduced cycle to cycle control for single input-single output systems, [1], and here it is extended to multiple input-multiple output systems. Gain selection, stability, and process noise amplification results are developed and compared with those obtained by previous researchers, showing good agreement. The limitation of imperfect knowledge of the plant model is then imposed. This is consistent with manufacturing environments where the cost and number of tests to determine a valid process model is desired to be minimal. The implications of this limitation are modes of response that are hidden from the controller. Their effects on system performance and stability are discussed.**

Index Terms—**Multivariable Control, Cycle to Cycle, Discrete Event.**

I. Introduction

CYCLE-TO-CYCLE (CtC) control for manufacturing processes has been proposed as a means of improving the statistical performance of unit processes. The name denotes that process measurements and subsequent control adjustments are only made between processing cycles. The prior work at MIT [2, 3, 4] was limited to single input-single output (SISO) processes, and did show great potential for process improvement. This paper considers the extension of CtC control to multiple input-multiple output (MIMO) systems.

Cycle-to-cycle control is a method for improving the performance of manufacturing processes that are inaccessible to measurements or control during the manufacturing cycle. This limitation stems from the impossibility, or the prohibitively high cost, of placing sensors and actuators that could result in in-process control. Examples of such processes are sheet metal forming and chemo-mechanical polishing (CMP) where proper measurements during a cycle are very difficult.

This work was supported in part by the Singapore MIT Alliance, Innovation in Manufacturing Systems and Technology Programme

Cycle-to-cycle control has been shown to be similar to run-by-run (RbR) control which uses an exponentially weighted moving average (EWMA) controller [3, 4]. However, cycle-to-cycle control has been developed from a linear discrete time control theory point of view. This different starting point allows one to make many strong statements about the stability and performance of systems under consideration while using predictive tools such as the discrete-time root locus diagram [5].

Figure 1 shows a generic discrete time multiple input-multiple output control block diagram. Note that the controller has been separated into two parts: the controller dynamics matrix G_c and the static controller gain matrix K_c.

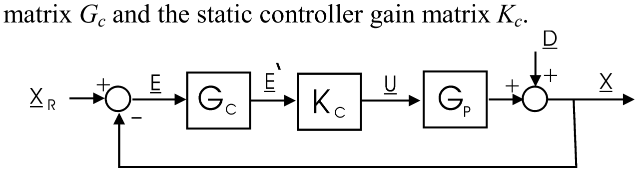

Figure 1 Generic multiple input-multiple output control system block diagram.

When applied to the simplest MIMO system (a *2x2* system) that still holds the properties of more complex systems (*nxn* systems), the elements take the following form:

$$G_c = \frac{z}{z-1} I$$
$$K_c = \begin{bmatrix} k_{c11} & k_{c12} \\ k_{c21} & k_{c22} \end{bmatrix} \quad (1)$$
$$G_p = \frac{1}{z} \begin{bmatrix} k_{11} & k_{12} \\ k_{21} & k_{22} \end{bmatrix}$$

where I is the identity matrix, z is the unit delay operator such that

$$x_{i-1} \equiv \frac{1}{z} x \quad (2)$$

and G_p is the plant model matrix with a one-cycle delay. This delay model results directly from the cycle to cycle assumption and the controller dynamics term G_c is an extension of the work of Hardt and Siu [3] who showed that this is the optimal controller form for SISO CtC.

II. BACKGROUND

The extension of single input-single output post-process feedback systems to multiple input-multiple output systems has been undertaken in the past [6, 7, 8, 9]. Key conclusions relating to the application of MIMO CtC control and control system analysis are reviewed below.

A. Controller Gain Selection

This development is separate but similar to the transfer function approach presented in Kosut *et al.* [6].

For most manufacturing processes, minimum settling time is highly desirable. For a discrete system, this can be represented by one-time step settling. This becomes the design goal for CtC control systems. Thus, a closed-loop transfer function, or the input-output relationship of the closed-loop system, should take the following form:

$$\underline{X} = \frac{1}{z}\underline{X}_R \Rightarrow \frac{\underline{X}}{\underline{X}_R} = \frac{1}{z}I \tag{3}$$

The closed-loop transfer function for the block diagram shown in Figure 1 may be written as:

$$[(z-1)I + G_P^* K_c]^{-1} G_p^* K_c = \frac{1}{z} I \tag{4}$$

where the scalar "dynamic" delay elements have been factored out as:

$$G_c = \frac{z}{z-1} I$$
$$G_c = \frac{z}{z-1} G_c^* \tag{5}$$
$$G_p = \frac{1}{z} G_p^*$$

In order for the equality to hold, i.e. to achieve the desired closed-loop transfer function, the following must be true:

$$G_P^* K_c = I \Rightarrow \begin{bmatrix} k_{11} & k_{12} \\ k_{21} & k_{22} \end{bmatrix} \begin{bmatrix} k_{c11} & k_{c12} \\ k_{c21} & k_{22} \end{bmatrix} = \begin{bmatrix} 1 & 0 \\ 0 & 1 \end{bmatrix} \tag{6}$$

Thus, given an invertible plant gain matrix G_p, the controller gain matrix needed to achieve one time-step settling is simply its inverse. An important observation resulting from this result is that this controller gain matrix will decouple a coupled process.

The same solution for the controller gain matrix is reached by Kosut *et al*. [6] and Edgar *et al*. [7].

B. Closed-Loop Stability

The stability limits of this system can be investigated by the use of the discrete-time root-locus [5]. The discrete-time root-locus relies on the z-plane representation of the stable region of a system. The stable region of the infinite z-plane consists of the interior of a unit circle centered at the origin. This region, along with constant damping and frequency, lines is shown in Figure 2. The center of the circle denotes one time-step settling. The outer boundary of the circle denotes infinite-time settling and defines the border between a stable and an unstable system. Thus, the relative stability of a system may be quantified as the distance away from this instability boundary.

The stability of a system is determined by the location of the roots of its characteristic equation:

$$\left|(z-1)I + G_P^* K_c\right| = 0 \tag{7}$$

For the special case where a decoupled system is achieved, but is not equal to the identity matrix because of a scaling factor, α:

$$G_P^* K_c = \alpha I \tag{8}$$

equation (7) may be employed to determine the stability limits of α:

$$0 < \alpha < 2 \tag{9}$$

This result is the same as obtained in Hardt and Siu [3] and Sachs *et al.* [10].

Employing equation (7) once again, it is possible to determine the stability of a system using any controller gain matrix, not necessarily a scaled inverse of the plant matrix. The characteristic equation of the system may be written in a familiar form:

$$|sI - A| = 0 \tag{10}$$

where:

$$A \equiv I - G_P^* K_c \tag{11}$$

Since the eigenvalues of A are also the poles of the closed loop system, the stability criteria is realized in another form:

$$eig(A) < 1 \tag{12}$$

This is the same result as presented in Kosut *et al*. [6].

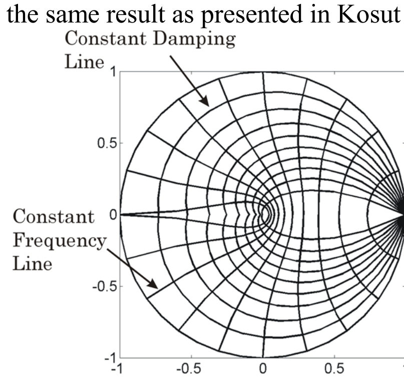

Figure 2 z-plane stable region with constant damping and frequency lines [5].

C. Process Noise Amplification

The use of closed-loop feedback changes the noise transmission properties of a system. An open-loop process is typically subject to random variations, which can be modeled here as a random output disturbance. When subject to CtC control this inherent process noise can be either attenuated or amplified depending on the degree of correlation of the noise process. Siu [2] and Hardt and Siu [3] have shown that the amount of noise amplification from CtC can be accurately predicted for single input-single output systems. This variance ratio $\frac{\sigma_{CtC}^2}{\sigma_n^2}$ for normal, identically distributed, independent (i.e. uncorrelated) (NIDI) noise is:

$$\frac{\sigma_{CtC}^2}{\sigma_n^2} = 1 + K\frac{1-(1-K)^{2(n-1)}}{(2-K)} \tag{13}$$

where K is the loop gain and n is the number of samples used to compute the variance ratio.

Box and Luceno, [8], also present a method for determining the amount of noise amplification at the output given an EWMA controller smoothing constant θ:

$$\theta = 1 - G \tag{14}$$

where G is the loop gain. Under the assumption that the disturbance can be represented by an integrated moving average (IMA) time series model with a smoothing constant θ_o (i.e. a non-stationary parameter $\lambda_o=1-\theta_o$ [8]) the result is:

$$\frac{\sigma_{out}^2}{\sigma_{in}^2} = 1 + \frac{(G-\lambda_o)^2}{G(2-G)} \tag{15}$$

Although these results seem different, they are actually the same when taken to their appropriate limits. In order to correspond with a NIDI disturbance, equation (15) must have $\lambda_o=0$. Also, since equation (15) is for an infinite series, equation (13) must have

$$n \to \infty \tag{16}$$

Noting the fact that, as stated in [8], $0<G<2$, and that G is equivalent to K, then:

$$\lim_{n\to\infty}\left(1-(1-K)^{2(n-1)}\right) = 1 \tag{17}$$

Substituting this equation into the previous results, one obtains the variance amplification for an infinite-number-of-measurements NIDI noise process:

$$\frac{\sigma_{out}^2}{\sigma_{in}^2} = 1 + \frac{G}{(2-G)} = 1 + \frac{K}{(2-K)} \tag{18}$$

Because of the decoupling nature of the ideal controller matrix presented in the previous section, these results obtained for single input-single output systems may be applied directly to multiple input-multiple output systems, i.e. a decoupled *nxn* MIMO system is equivalent to *n* independent SISO systems.

III. Process Model

As introduced in Rzepniewski and Hardt, [1], and repeated in equation (1), the plant model Gp is a gain and delay combination. Even given the simple structure of the required model, appropriate approximations need to be made to determine models for large numbers of coupled inputs and outputs. Linear models for single input-single output (SISO) systems are simple to get with only a few tests. Linear models for multiple input-multiple output systems require secondary assumptions and approximations to establish a good model with only a few tests. A system with n^2 inputs and n^2 outputs requires n^4 coefficients to satisfy the matrix form of the CtC model:

$$\begin{bmatrix} \vdots \\ n^2 \\ \vdots \end{bmatrix}_{OUTPUTS} = \left[n^2 x n^2\right]_{GAINS} \begin{bmatrix} \vdots \\ n^2 \\ \vdots \end{bmatrix}_{INPUTS} \tag{19}$$

Even with the realization that each test gives a potential of n^2 data points, n^2 tests are still required to fill the gain matrix; for a modest size system with 144 inputs, 144 tests would be required to determine the gain matrix. Thus, for systems with non-trivial dimensionality, the number of tests required to independently identify each entry of the gain matrix is not suitable for manufacturing environments.

Because of the large number of tests required to establish the gain matrix for systems with high numbers of inputs and outputs, approximations need to be made. Rzepniewski and Hardt, [1], introduce a Gaussian model approximation to describe the influence that an input has on the neighboring outputs. This model is shown to adequately describe a class of processes where the influence of the inputs on the outputs is diffusive in nature. Examples of such processes include chemo-mechanical polishing (CMP), heating, and discrete-die sheet metal forming.

IV. Performance Limitations

As noted previously, knowledge of the plant gain matrix allows the design of a perfect decoupling controller matrix. However, the only way a perfect controller matrix can be designed for a physical system is through perfect knowledge of the physical plant via the gain matrix G_p. As explained in the previous section, this is not practical. Thus, the theoretical performance predictions developed thus far, which are based on knowledge of the ideal plant, need to reflect this limitation.

A. Eigenvalue Location

The first effect of using a non-ideal plant matrix is a change in the eigenvalue locations. As introduced in equations (7) and (10), the eigenvalues of a system are the roots of the characteristic equation and determine the homogenous response of a system. Because the origin of the *z*-plane indicates one time-step settling, it is desirable to have all eigenvalues located there. Note that this is the result obtained when using a controller matrix that is the inverse of the plant matrix. Unless the product of the plant and gain matrices results in the identity matrix, the eigenvalues of the system will not be at the origin.

To investigate the effects of imperfect plant knowledge, a 5,000 count Monte Carlo simulation was implemented for a process gain matrix with weak coupling (small off-diagonal terms):

$$K_P = \begin{bmatrix} 1 & 0.1 \\ 0.1 & 1 \end{bmatrix} \tag{20}$$

The controller gains are selected by the inverse method assuming the above process matrix. Following the calculation of the controller matrix, the process matrix is perturbed by independently adding normally distributed perturbations, zero mean and 0.01 variance, to each of the matrix entries:

$$K_P = \begin{bmatrix} 1 & 0.1 \\ 0.1 & 1 \end{bmatrix} + \begin{bmatrix} \Delta_{11} & \Delta_{12} \\ \Delta_{21} & \Delta_{22} \end{bmatrix} = \begin{bmatrix} 1+\Delta_{11} & 0.1+\Delta_{12} \\ 0.1+\Delta_{21} & 1+\Delta_{22} \end{bmatrix} \tag{21}$$

where $\Delta_{11} \neq \Delta_{12} \neq \Delta_{21} \neq \Delta_{22}$. Note that one standard deviation represents from 10 to 100 percent of the matrix entries.

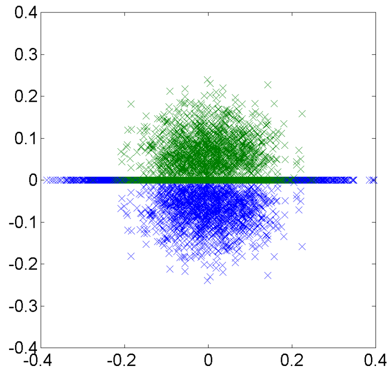

Figure 3 Eigenvalue location on the z-plane.

Figure 3 shows the location of the system eigenvalues in the complex *z*-plane. It is apparent that the poles largely remain on the real axis. The settling time may be calculated using the definition of the *z*-transform and the well accepted approximation for settling to within 2 percent of the input:

$$t_s = \frac{4}{\sigma} \tag{22}$$

where σ is the real-axis coordinate in the s-plane [5]. The homogenous response settling time, in terms of cycles, then becomes:

$$t_s = \frac{-4}{\ln(r)} \tag{23}$$

where *r* is the distance from the origin of the z-plane. A review of Figure 3 shows that over 90% of simulated poles lie within a three cycle radius of *r=0.26*.

B. Transmission Zeros

The second effect of imperfect plant knowledge is the appearance of transmission zeros, or modes of operation which are hidden from the controller. The zeros affect the forced response of a system. To investigate the origin of transmission zeros, one must look at the closed-loop transfer function:

$$\frac{\underline{X}}{\underline{X}_R} = \frac{1}{\det\left|(z-1)I + G_P^* K_c\right|} Adj\left[(z-1)I + G_P^* K_c\right] G_P^* K_c \tag{24}$$

For a *2x2* system with eigenvalues located at the origin, the above equation may be expanded to:

$$\frac{1}{z^2}\begin{bmatrix} (k_{c11}k_{11} + k_{c21}k_{12})(z-1) + (k_{11}k_{22} - k_{12}k_{21})(k_{c11}k_{c22} - k_{c12}k_{c21}) & (k_{c12}k_{11} + k_{c22}k_{12})(z-1) \\ (k_{c11}k_{21} + k_{c21}k_{22})(z-1) & (k_{c12}k_{21} + k_{c22}k_{22})(z-1) + (k_{11}k_{22} - k_{12}k_{21})(k_{c11}k_{c22} - k_{c12}k_{c21}) \end{bmatrix} \tag{25}$$

To achieve the desired transfer function of equation (3), the coefficients of the diagonal *(z-1)* terms and the determinant of the controller and plant matrices must equal 1. The coefficients of the off-diagonal terms must also equal *0*. These requirements cannot be satisfied with imperfect knowledge of the plant matrix. The implication of this is that certain system modes will not be controllable and the system will have undesirable forced response properties.

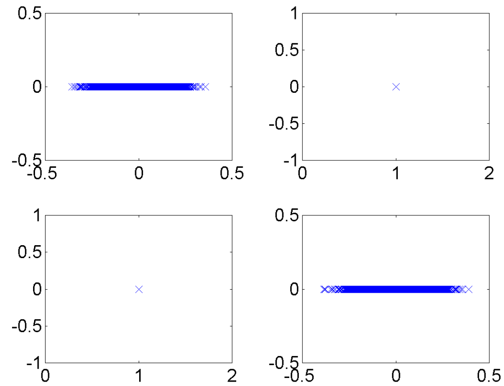

Figure 4 System zeros shown according to their location within the closed-loop transfer function matrix.

The system of equations (20) and (21) is used to examine the movement of these closed-loop zeros. Figure 4 shows the results obtained from 5,000 simulations. Note that the zeros are shown according to their location in the closed-loop transfer matrix. Note that this separation of the homogenous and forced response is a property unique to MIMO systems. SISO system response is fully determined by the locations of the poles.

C. Simulation example

The influence of the movement of the system zeros is best explained by example. A candidate MIMO process matrix is chosen:

$$K_P = \begin{bmatrix} 2 & 3 \\ 5 & 7 \end{bmatrix} \tag{26}$$

Since the characteristic equation contains only two coefficients that determine the pole locations and the candidate *2x2* system has four controller gains to be determined, there exists and infinite set of solutions that yield the desired eigenvalue locations. To simplify analysis, a diagonal controller matrix form is chosen and the eigenvalues are set to zero. Note that this is not necessarily the same as having imperfect knowledge of the plant. This simplification is done only to emphasize the effects of transmission zeros.

The calculation of a diagonal controller with eigenvalues located at the origin results in two solutions which are presented in Table 1. The closed-loop transfer function matrix is included, thus showing the system zeros. Note that the form of the response is determined by both the location of the zero and a magnitude scaling.

Controller Gain Matrix	Closed-Loop Transfer Function Matrix
$\begin{bmatrix} -1.44 & 0 \\ 0 & 0.70 \end{bmatrix}$	$\frac{1}{z^2}\begin{bmatrix} -2.87z+3.87 & 2.09(z-1) \\ -7.18(z-1) & 4.83z-3.87 \end{bmatrix}$
$\begin{bmatrix} 2.44 & 0 \\ 0 & -0.41 \end{bmatrix}$	$\frac{1}{z^2}\begin{bmatrix} 4.87z-3.873 & -1.23(z-1) \\ 12.18(z-1) & -2.87z+3.87 \end{bmatrix}$

Table 1 Controller gains and transfer function matrices for simulation example.

Figure 5 and Figure 6 show the ideal and non-ideal responses of the candidate system, respectively. Note that an inverse-of-the-plant controller matrix is used to calculate Figure 5 and the second of the two solutions in Table 1 is used in Figure 6. Also note that the simulated environment is noise-free.

The effect of transmission zeros on the forced response of the system is clearly visible in Figure 6. The change in inputs (forcing) causes the appearance of a hidden mode which causes a large deviation from the input. This mode quickly disappears once the input is held steady (no forcing) and only the homogenous response remains. As predicted, the homogenous response shows one time-step settling.

Thus, the appearance of transmission zeros is undesirable for systems that require continuous adjustments (forcing).

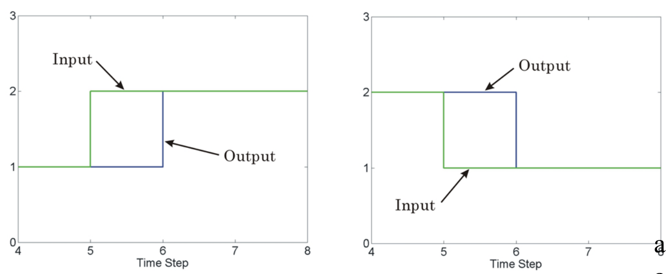

Figure 5 Ideal system response obtained through perfect plant knowledge.

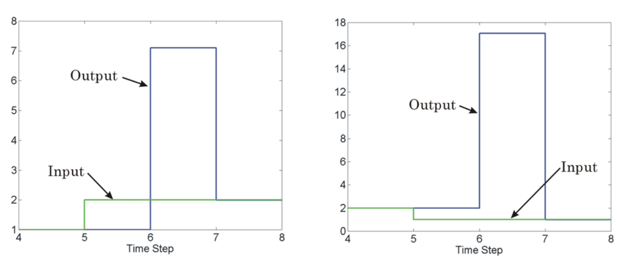

Figure 6 Influence of transmission zeros on the closed-loop response of a system.

V. MIMO PROCESS NOISE AMPLIFICATION

In light of the effects of transmission zeros, the process noise amplification predictions are investigated using simulation. The nominal plant matrix of equation (20) is used:

$$K_P = \begin{bmatrix} 1 & 0.1 \\ 0.1 & 1 \end{bmatrix} \tag{27}$$

Once again, the controller matrix is designed by taking the plant inverse. If the nominal process matrix is used in the simulation this will yield a fully decoupled system. To display non-trivial, coupled results, the plant matrix is perturbed without readjusting the controller gain matrix, according to:

$$K_P = \begin{bmatrix} 1 & 0.1 \\ 0.1 & 1 \end{bmatrix} + \begin{bmatrix} \Delta_{11} & \Delta_{12} \\ \Delta_{21} & \Delta_{22} \end{bmatrix} \tag{28}$$

The perturbations are zero mean with a standard deviation of 0.1. The perturbed plant matrix is then used in a simulation of 5,000 cycles subject to additive noise at the process output, as shown in Figure 1. Analytical results are computed using equations (13) and (15) for correlated and non-correlated noise, respectively. These analytical formulas are termed SISO results since they rely on the decoupling of the MIMO system into many SISO systems through the controller gain matrix.

Figure 7 shows the results obtained from 1,000 realizations of the perturbed MIMO plant matrix. It can be seen that the MIMO case closely follows the predicted SISO response for a unity loop gain. Also, the variance amplification ratio appears to be lower than predicted for gains above one.

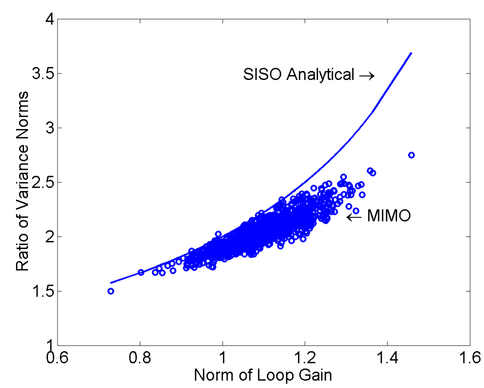

Figure 7 Uncorrelated (NIDI) process noise amplification results.

Tests are also carried out to determine the noise-amplification effects of correlated, non-NIDI, noise. To achieve correlation, the NIDI noise is passed through a correlating filter of the form:

$$\frac{1-P}{z-P} \tag{29}$$

where $P=0.8$ for the presented case. Figure 8 shows simulation results from 1,000 iterations of the perturbed process matrix. Once again, the appearance of transmission zeros causes a small deviation from theoretical predictions. In addition, the variance amplification ratio is lower than predicted by theory.

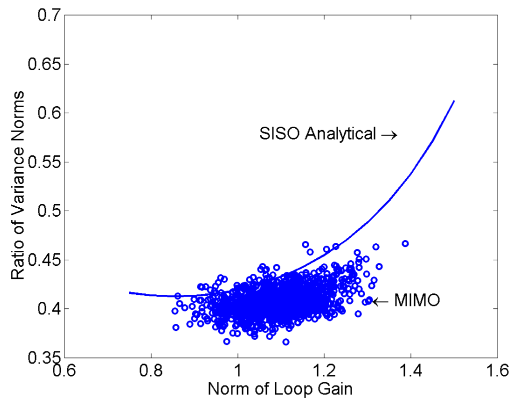

Figure 8 Correlated (non-NIDI) process noise amplification results.

VI. Plant Misidentification

In section III a limitation on the ability to properly identify a plant gain matrix was imposed. This limitation influences the controller's ability to take the ideal control action and thus causes a slower settling time. These effects are studied through simulation in this section.

Once again, the plant matrix of equation (20) is used. The controller is based on this ideal matrix, by taking its inverse, and is not adjusted as the plant matrix is perturbed. A process is considered settled when the output has reached within 2 percent of the input.

First, the case of pre-process plant misidentification is examined. Note that the process gain is assumed to stay constant until settling is achieved, however this ideal gain is not known fully when the controller is designed. Figure 9 shows the percent of processes that settled within two cycles as a function of the standard deviation of the perturbations. Each data point on the formed line represents 5,000 independent trials. One can observe that up to approximately 0.09 standard deviations there is little penalty for plant misidentification. This shows that the system is robust to pre-process plant misidentification.

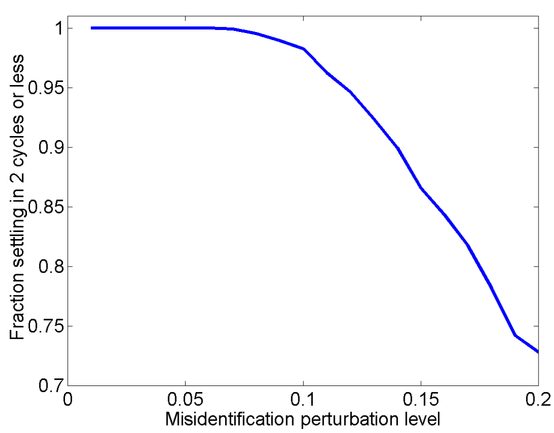

Figure 9 Percentage of systems settling in 2 cycles or less as a function of misidentification level.

The case of between-cycles plant misidentification is examined. This may occur when a new workpiece is introduced for each control cycle. Note that the process gain is assumed to vary after each cycle until settling is achieved. Figure 10 shows the percent of processes that settled within two time steps as a function of the standard deviation of the perturbations. Once again, each data point on the formed line represents 5,000 independent trials. One can observe that there are more severe penalties for misidentifying the gain matrix during the process. The curve had a downward slope from the very lowest level of noise and it is higher than the slope observed in Figure 10. One can see that a standard deviation of 0.08 in plant misidentification now causes only 43 percent of the processes to settle within two time steps.

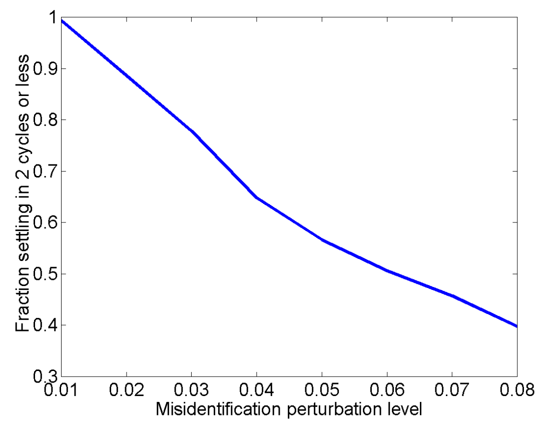

Figure 10 Percentage of systems settling in 2 cycles or less as a function of misidentification level.

VII. Conclusion

This paper provides an extension of the Cycle to Cycle control concept to a general multivariable case. It has been shown that the properties of zero mean error and bounded variance amplification that were seen for the SISO case can also be achieved for the MIMO case. A design procedure is presented to achieve this ideal result. However, the MIMO control case is more sensitive to modeling errors, which are inherent in practical manufacturing applications. The knowledge of these effects, presented here as undesirable transmission zeros and slower than desired settling times, is critical in designing a universal, robust MIMO cycle to cycle control scheme.

References

1 Rzepniewski, A.K., Hardt, D.E., *Gaussian Distribution Approximation for Localized Effects of Input Parameters*. Second Annual SMA Symposium, Singapore, Jan. 2003.

2 Siu, G. T.-S., *Cycle to Cycle Feedback Control of Manufacturing Processes*. SM Thesis in Mechanical Engineering, MIT, Feb. 2001.

3 Hardt, D.E., Siu, T.-S., *Cycle to Cycle Manufacturing Process Control*. First Annual SMA Symposium, Singapore, Jan. 2002.

4 Hardt, D.E., Rzepniewski, A., Pi, A., *Cycle-to-Cycle Feedback Control and its Application to Sheet Metal*

Forming. Proceedings of the JSME/ASME International Conference on Materials and Processing, Oct. 2002.

5 Kuo, B. C., *Automatic Control Systems*. Englewood Cliffs: Prentice-Hall, 1995.

6 Kosut, R. L., de Roover, D., Emami-Naeini, A., Ebert, J. L., *Run-to-Run Control of Static Systems*. Proceedings of the 37th IEEE Conference on Decision and Control, 1998, pp. 695-700.

7 Edgar, T.F., Campbell, W.J., Bode, C., *Model-Based Control in Microelectronics Manufacturing*. Proceedings of the 38th IEEE Conference on Decision and Control, 1999, pp. 4185-4191.

8 Box, G., Luceno, A., *Statistical Control by Monitoring and Feedback Adjustment*. New York: Wiley-Interscience, 1997.

9 Moyne, J., ed., del Castillo, E., ed., Hurwitz, A., M., ed. *Run-to-Run Control in Semiconductor Manufacturing*. Boca Raton: CRC Press LLC, 2001.

10 Sachs, E., Hu, A., Ingolfsson, A., *Run by Run Process Control: Combining SPC and Feedback Control*. IEEE Transactions on Semiconductor Manufacturing, 1995, vol. 8, no. 1, pp. 26-43.